

# Nanoscale magnetic structure of ferromagnet/antiferromagnet manganite multilayers

D. Niebieskikwiat and M.B. Salamon

*Department of Physics, University of Illinois at Urbana-Champaign, Urbana, Illinois 61801, USA*

L.E. Hueso and N.D. Mathur

*Department of Materials Science, University of Cambridge, Cambridge CB2 3QZ, UK*

J.A. Borchers

*NIST Center for Neutron Research, National Institute of Standards and Technology, Gaithersburg, Maryland 20899, USA*

Polarized Neutron Reflectometry and magnetometry measurements have been used to obtain a comprehensive picture of the magnetic structure of a series of  $\text{La}_{2/3}\text{Sr}_{1/3}\text{MnO}_3/\text{Pr}_{2/3}\text{Ca}_{1/3}\text{MnO}_3$  (LSMO/PCMO) superlattices, with varying thickness of the antiferromagnetic (AFM) PCMO layers ( $0 \leq t_A \leq 7.6$  nm). While LSMO presents a few magnetically frustrated monolayers at the interfaces with PCMO, in the latter a magnetic contribution due to FM inclusions within the AFM matrix was found to be maximized at  $t_A \sim 3$  nm. This enhancement of the FM moment occurs at the matching between layer thickness and cluster size, where the FM clusters would find the optimal strain conditions to be accommodated within the “non-FM” material. These results have important implications for tuning phase separation via the explicit control of strain.

PACS numbers: 75.70.Cn, 75.70.Kw, 61.12.Ha

Nanostructured magnetic materials are already finding applications in magnetic recording and magnetic memory devices. One important focus has been on tunneling magnetoresistance (TMR), in which ferromagnetic (FM) layers having spin-polarized conduction electrons are separated by a non-magnetic insulating barrier [1, 2]. Double-exchange magnets such as  $\text{La}_{2/3}\text{Sr}_{1/3}\text{MnO}_3$  and  $\text{La}_{2/3}\text{Ca}_{1/3}\text{MnO}_3$ , because of their high degree of spin polarization, have been considered as the metallic layers along with various insulating barriers such as  $\text{SrTiO}_3$  (STO),  $\text{LaAlO}_3$ , and  $\text{NdGaO}_3$ . Results have not been encouraging. One possible problem with these systems lies in the interfacial magnetization, which may fall off more rapidly with increasing temperature than does the bulk magnetization [2].

As a different approach to TMR devices, we have fabricated all-manganite multilayers utilizing antiferromagnetic (AFM) insulating manganites as the barrier [3, 4, 5, 6]. Our goal is to study the magnetic properties of such multilayers with special attention to two different aspects. First, we expect that the similarities in lattice structure and stoichiometry at the manganite-manganite interfaces will minimize the suppression of interfacial magnetization. Second, we explore the possibility of inducing magnetization in the AFM spacer and thereby having a magnetic-field-sensitive tunneling barrier, which would contribute to the TMR effect. AFM materials with FM instabilities, i.e. phase-separated manganites, are thus ideal candidates for the insulating layers [7].

We have chosen as the barrier layer  $\text{Pr}_{2/3}\text{Ca}_{1/3}\text{MnO}_3$  (PCMO), which is AFM and insulating, but supports nanoscale FM droplets within the AFM matrix [8, 9, 10]. Because of its high Curie temperature, we use

$\text{La}_{2/3}\text{Sr}_{1/3}\text{MnO}_3$  (LSMO) for the FM layers. We report the magnetic properties as functions of temperature and spacer-layer thickness, using Polarized Neutron Reflectivity (PNR) to map the magnetization profile through the multilayer structure. Despite the structural regularity of the interfaces, we find that magnetically disordered regions appear at the surfaces of the LSMO layers. Contrastingly, an enhanced FM moment is induced within the PCMO spacer when its layer thickness is  $\sim 3$  nm. Interestingly, this corresponds to the situation where the layer thickness matches the size of the FM clusters that occur in PCMO.

High quality epitaxial superlattices were grown on atomically flat STO (001) substrates by pulsed laser deposition at 750 °C. Then, the films were annealed at the same temperature in 60 kPa of oxygen for 1 h. The multilayers involve five repetitions of LSMO/PCMO bilayers, with LSMO as the starting layer. We prepared seven different films, where the LSMO thickness is in all cases 11.9 nm and the thickness of PCMO is  $t_A = 0, 0.8, 1.7, 2.7, 3.5, 4.3$ , and 7.6 nm, respectively (for  $t_A = 0$ , a single 11.9-nm-thick layer of LSMO was grown). The out-of-plane lattice parameters (3.85 and 3.76 Å for LSMO and PCMO, respectively) are smaller than the bulk values (3.88 and 3.83 Å, respectively), confirming the tensile stress imposed by the substrate (the in-plane lattice parameter is 3.90 Å for all STO, LSMO, and PCMO).

Magnetization ( $M$ ) data were obtained in a superconducting quantum interference device (SQUID) magnetometer, with in-plane magnetic fields  $\mu_0 H \leq 7$  T.  $M(H)$  loops at a temperature  $T = 5$  K for three selected samples are shown in Fig. 1. All our multilayers show sharp FM loops, with a Curie temperature  $T_C \sim 345$  K (obtained from  $M$  vs  $T$ ) corresponding to the LSMO layers.

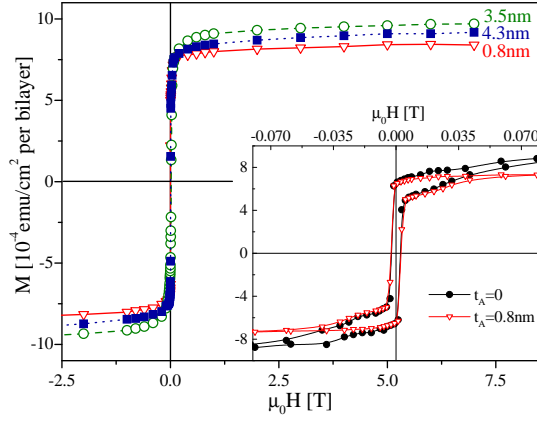


FIG. 1: (Color online) Magnetization loops at  $T = 5$  K for three selected samples ( $1 \text{ emu} = 10^{-3} \text{ A m}^2$ ). The labels indicate the thickness of the  $\text{Pr}_{2/3}\text{Ca}_{1/3}\text{MnO}_3$  layers ( $t_A$ ). Inset: low-field region of the same loops for  $t_A = 0$  and  $0.8$  nm.

A close inspection to these data reveals a small but clear variation of the magnetic moment with the thickness  $t_A$ . After correcting for a minor substrate contribution [11], we obtained the spontaneous magnetization of the samples ( $M_0$ , the back-extrapolation to  $H = 0$  from the high-field saturated region). Since only FM phases can give a spontaneous moment,  $M_0$  is a direct measure of the FM volume of the samples [12]. Two curious features can be noticed in the  $M_0$  vs  $t_A$  curve [Fig. 2(a)]. At  $t_A = 0$ ,  $M_0$  corresponds to the saturation of pure LSMO, but then the moment decreases when a thin layer of PCMO ( $t_A = 0.8$  nm) is added between the LSMO layers. The decrease of  $M_0$  suggests a reduction of the magnetic moment within the LSMO layers, since any FM contribution from the PCMO should align parallel to the applied field (this is indeed confirmed by PNR). For thicker PCMO layers  $M_0$  increases again due to the contribution of FM droplets inside the PCMO [3, 7, 8, 9, 10].

Among the interactions that could lead to the reduction of  $M_0$ , an AFM coupling between different LSMO layers can be ruled out. On one hand, RKKY-like interactions require a non-magnetic metal as the intermediate layer [13], which is not the case of PCMO. On the other hand, the weak dipolar interactions could hardly be responsible for this behavior, and the applied fields should re-align the magnetic moments of the different LSMO layers. However,  $M$  stays the same even after cooling the samples under a high field of 7 T. Differently, a plausible reason for the reduction of  $M_0$  is the formation of magnetically disordered regions at the LSMO side of the FM-AFM interfaces. Indeed, interface regions with degraded magnetization have been observed in a number of different systems [2, 14, 15].

While magnetization measurements cannot be conclusive about the origin of the reduction of  $M_0$ , Polarized

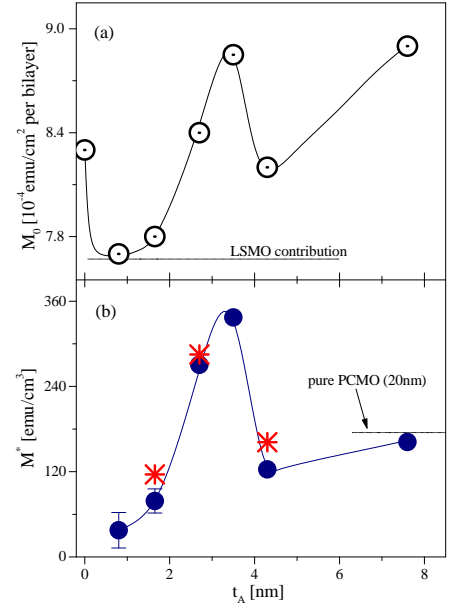


FIG. 2: (Color online) (a) Total FM moment of the samples at 5 K as a function of  $t_A$ . The horizontal line is the estimated contribution of the LSMO layers for  $t_A > 0$ . (b) FM moment of the  $\text{Pr}_{2/3}\text{Ca}_{1/3}\text{MnO}_3$  layers only. The dotted line shows the FM moment of a 20-nm-thick PCMO film. The FM moment obtained from PNR at 6 K is also shown (star symbols).

Neutron Reflectivity provides a depth profile of  $M$  and is thus an ideal tool to test for the existence of disordered interfaces [14, 15]. PNR experiments were carried out on the NG1 reflectometer at the NIST Center for Neutron Research (NCNR) at  $T = 6, 120$ , and  $300$  K on three selected samples,  $t_A = 1.7, 2.7$ , and  $4.3$  nm. An in-plane magnetic field of  $0.32$  T was applied, enough to reach the saturation of the films (see Fig. 1). Spin-flip scattering, which is indicative of magnetization perpendicular to the applied field, was thus not observed. As typical examples, the top panels of Fig. 3 show the non-spin flip reflectivities ( $R^{++}$  for spin up and  $R^{--}$  for spin down) for  $t_A = 2.7$  nm at  $300$  K and for  $t_A = 4.3$  nm at  $6$  K (for the sake of clarity  $R^{--}$  was multiplied by 10). Note that the splitting between the non-spin flip reflectivities is related to the projection of the magnetic moment parallel to the applied field. Using the *Reftpak* software suite [16], the data were fitted to models for the depth profile of the structure and magnetization after correcting for polarization efficiencies ( $> 97\%$ ) and other instrumental effects. The models used to fit these data were kept as simple as possible, while keeping a high quality fit. We must mention that the statistical quality of the PNR data for  $t_A = 1.7$  nm is not as good as for the other two samples studied, likely because of the small thickness of PCMO. However, we note that these data were successfully fitted with parameters that are consistent with the magnetization results as well as with the other two samples (see

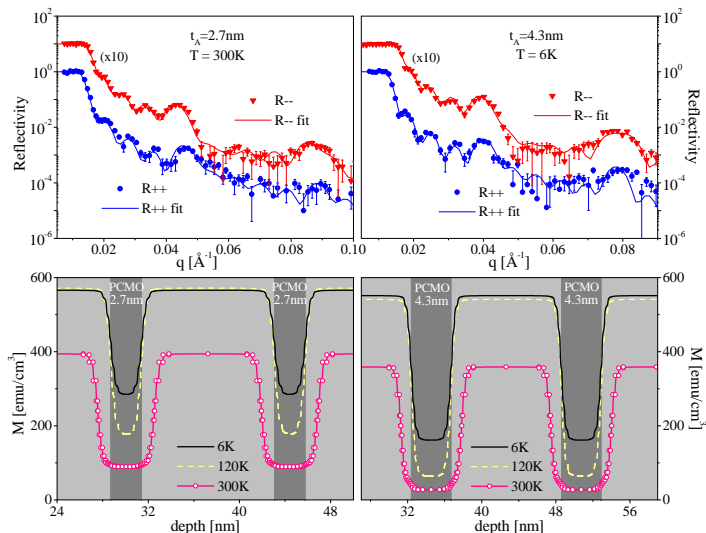


FIG. 3: (Color online) Top: Neutron reflectivity spectra for the samples with  $t_A = 2.7$  nm (at  $T = 300$  K, left), and  $t_A = 4.3$  nm (at  $T = 6$  K, right). The triangles and circles correspond to the  $R^-$  and  $R^{++}$  reflectivity data, respectively ( $R^-$  was multiplied by 10). The solid lines through the data are the corresponding fits. Bottom: magnetization profiles at the three studied temperatures (as labeled) for the same samples ( $t_A = 2.7$  and  $4.3$  nm on the left and right sides, respectively). The light and dark gray areas are the LSMO and PCMO layers, respectively.

results below). The obtained  $M$  profiles for  $t_A = 2.7$  and  $4.3$  nm are shown in the bottom panels of Fig. 3. For all three samples, the fits at  $T = 300$  K unambiguously show the presence of 1.2-nm-thick regions on the LSMO side of the interfaces where  $M$  is widely suppressed as compared to the inner part of the LSMO layers, the so-called magnetically disordered interfaces (MDIs). Although these MDIs are easily distinguished at 300 K, at low  $T$  they do not show up very clearly. However, based on the drop of  $M_0$  at 5 K between the pure LSMO sample ( $t_A = 0$ ) and  $t_A = 0.8$  nm [Fig. 2(a)], we estimate an effective thickness of  $\sim 0.5$  nm for these interface regions. This size is comparable to the roughness of the interfaces and to the depth resolution limits of PNR, which could mask the reduced magnetization on this lengthscale.

MDIs were previously observed in several magnetic heterostructures, including superlattices with FM-manganite layers [14, 15]. However, more striking is the presence of disordered regions at the free surfaces of manganite samples [17, 18]. It has been argued that the lower atomic coordination caused by the surface termination of the crystal structure lowers the effective magnetic interactions, leading to a degraded magnetization [17]. In  $\text{La}_{0.7}\text{Sr}_{0.3}\text{MnO}_3$  films, spin-resolved photoemission spectroscopy (SPES) experiments show that, while at low  $T$  full saturation is reached, at higher  $T$  (below  $T_C$ ) several Mn-O layers at the free surface of the film exhibit a

reduced magnetization as compared to the material underneath [17]. This agrees with the general observation that the MDIs are in fact regions where  $M$  decays faster with  $T$ , and as a consequence the TMR becomes deteriorated [2]. Indeed, also in our PNR experiments the MDIs are more clearly observed at higher  $T$  (see Fig. 3). Notwithstanding this, we believe that even at low  $T$  these disordered interface regions give rise to anomalous features in our  $M(H)$  measurements. As shown in the inset of Fig. 1 for  $t_A = 0$  and  $0.8$  nm, the reversal of  $M$  when  $H$  changes sign consists of two steps: first a fast reversal occurs at  $\mu_0 H < 5$  mT, followed by a more gradual moment increase at higher fields. For both samples the fast reversal is similar, with the same values of  $M$ . However, at higher fields the magnetization for  $t_A = 0.8$  nm stays clearly lower than for  $t_A = 0$ , indicating that a full saturation of  $M$  is not reached. Since the difference between the two samples is the contact of the LSMO surfaces with PCMO, this behavior must be related to the interfaces. We conclude that the sharp reversal corresponds to the inner volume of LSMO in the films, while the gradual increase of  $M$  is related to the alignment of the disordered LSMO surfaces. At low  $T$ , full saturation can be reached in the free LSMO surface in high magnetic fields, as observed in the SPES experiments [17]. However, when the PCMO layers are put in contact with the LSMO surfaces, MDIs remain disordered in fields as large as 7 T and the magnetic moment is smaller (inset of Fig. 1). We thus speculate that the PCMO moments at the interfaces pin the magnetic moments of the already disordered LSMO surfaces.

Due to the existence of these MDIs, the FM contribution of the LSMO layers to the magnetic moment of the superlattices [dotted line in Fig. 2(a)] is smaller than the saturation in the pure LSMO film ( $t_A = 0$ ). This leads to the initial drop of  $M_0$  at low  $t_A$  clearly seen in Fig. 2(a). As the thickness of PCMO increases, the FM moment increases again and a second peculiar feature develops, i.e. a maximum of  $M_0$  at intermediate  $t_A$ . It is well known that PCMO is a phase separated manganite, either in bulk or thin film samples [8, 9, 10]. Indeed, we also prepared a 20-nm-thick PCMO film which exhibits spontaneous ferromagnetism. Its FM moment  $\sim 175$  emu/cm<sup>3</sup> appears superposed to the linear  $M$ - $H$  response of the predominant AFM background. In the multilayers, the FM moment of the PCMO layers can be obtained after subtracting the contribution from the LSMO [ $\sim 7.7 \times 10^{-4}$  emu/cm<sup>2</sup> each layer, dotted line in Fig. 2(a)]. The obtained FM contribution of the PCMO layers ( $M^*$ ) is plotted in Fig. 2(b) as a function of  $t_A$ .

The maximum of  $M_0$  now appears as a maximum in  $M^*$  vs  $t_A$ . For very small  $t_A$  values ( $< 2$  nm) the FM moment of PCMO remains small, below 80 emu/cm<sup>3</sup>. Presumably, the thin PCMO layers are not large enough to accommodate FM clusters, and only a small number of them can form. For large  $t_A$ ,  $M^*$  approaches the mag-

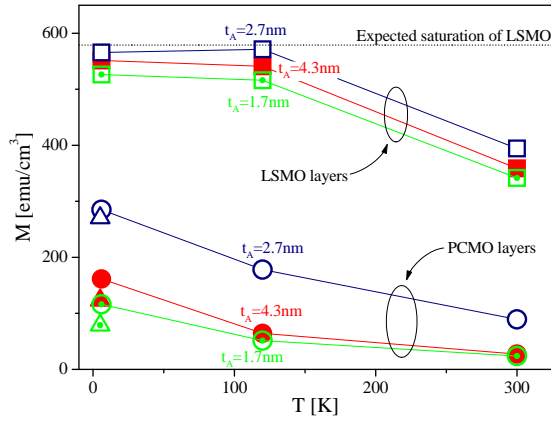


FIG. 4: (Color online) Temperature dependence of the FM moment of the different layers of the LSMO/PCMO superlattices, as obtained from PNR. The triangles are the magnetic moments of the PCMO layers deduced from the magnetization measurements at  $T = 5$  K [ $M^*$ , see Fig. 2(b)].

netic moment of the pure PCMO film (thickness 20 nm), as shown in Fig. 2(b). In between, the pronounced peak of  $M^*$  at  $t_A$  around 3 nm is also confirmed by the PNR experiments. When we compare the magnetic profiles of the samples at  $T = 6$  K, the magnetization in the LSMO layers is observed to be the same, and corresponds to the saturation of LSMO (solid lines in the bottom panels of Fig. 3). The temperature dependence of  $M$  in the LSMO layers is also the same for all the samples (square symbols in Fig. 4). However, the FM moment inside the PCMO layers is clearly larger in the 2.7 nm sample. Moreover, as demonstrated in Figs. 2(b) and 4, the values obtained from the PNR fits at 6 K are in perfect agreement with those calculated from  $M(H)$  at 5 K. This maximum FM contribution of the PCMO layers may originate from an overpopulation of FM clusters within the AFM matrix. Of course, PNR does not show this *in-layer* nanoscale structure since the depth-dependent  $M$  profile represents an average of the FM moment across the film plane.

The cause of such an increase of the FM moment of PCMO is not obvious. The proximity of the FM LSMO layers could act as an internal field [5, 19], raising the number of FM droplets. This proximity effect would be related to a strong influence of the FM layers on the AFM ones, mediated by interface magnetic interactions [15]. However, as we have already demonstrated the LSMO interfaces are magnetically degraded, thus making difficult any kind of interlayer magnetic coupling. This is especially clear at  $T = 300$  K, where the LSMO layers show 1.2-nm-thick MDIs and the overshooting of the FM moment in the PCMO for  $t_A = 2.7$  nm persists (Figs. 3 and 4). On the other hand, strain effects could play a major role in this behavior. Strain fields have been linked with nanoscale phase separation in a number of materials, including manganite thin films [9, 20]. In bulk PCMO sam-

ples the ground state is a mainly charge-ordered (CO) AFM phase [7]. On the contrary, while thin films are still AFM the CO state is not realized [4, 5, 19, 21]. Due to the strong electron-phonon coupling, strain fields play a key role in the CO phase. Then, the absence of charge ordering is likely related to the lattice strain and interface clamping in thin film samples. In  $\text{Pr}_{2/3}\text{Ca}_{1/3}\text{MnO}_3$ , the suppression of the CO phase could make the material especially unstable against the formation of FM clusters. Indeed, it is highly unusual that the FM contribution in the PCMO layers persists even at high  $T$  (300 K), as shown in Figs. 3 and 4. On the contrary, at this  $T$  a FM response is totally absent in bulk samples, confirming that strain fields must play a fundamental role in the stabilization of FM nanoclusters in our films. Likely, a matching condition between layer thickness and cluster size is responsible for the maximum FM moment of the PCMO layers at  $t_A \sim 3$  nm. Indeed, neutron scattering experiments show a similar lengthscale for the typical FM cluster size [10]. The accommodation of nanometric droplets in a strain field occurring at a similar lengthscale would favor an overpopulation of FM clusters.

In summary, the combination of PNR and magnetometry allowed us to reveal the nanoscale magnetic structure of the LSMO/PCMO multilayers. The stacking of PCMO on top of LSMO hampers the saturation at the surfaces of the ferromagnetic LSMO layers, which show 1.2-nm-thick magnetically disordered interfaces at 300 K. In the phase separated PCMO, a maximum FM moment occurs for layer thicknesses comparable to the characteristic lengthscale of the FM nanoclusters, i.e. for  $t_A \sim 3$  nm. This enhancement of ferromagnetism in the nominally AFM spacer could have important implications for the TMR response of these devices. In similar manganite multilayers an enhanced TMR was shown to be related to a partial metallization of the insulating layers at intermediate optimal thicknesses [3, 4]. In our superlattices, the maximum FM moment would also imply a tendency towards the metallization of the PCMO spacer, achieved through the specific control of strain.

- 
- [1] M. Ziese, Rep. Prog. Phys. **65**, 143 (2002).
  - [2] M. Viret *et al.*, Europhys. Lett. **39**, 545 (1997); M.-H. Jo *et al.*, Appl. Phys. Lett. **75**, 3689 (1999); V. Garcia *et al.*, Phys. Rev. B **69**, 052403 (2004); M.-H. Jo *et al.*, *ibid* **61**, R14905 (2000); Y. Lu *et al.*, *ibid* **54**, R8357 (1996).
  - [3] R. Cheng *et al.*, Appl. Phys. Lett. **72**, 2475 (1998).
  - [4] H. Li *et al.*, Appl. Phys. Lett. **80**, 628 (2002); A. Venimadhav *et al.*, J. Phys. D **33**, 2921 (2000).
  - [5] I.N. Krivorotov *et al.*, Phys. Rev. Lett. **86**, 5779 (2001).
  - [6] M.-H. Jo *et al.*, J. Phys.: Condens. Matter **15**, 5243 (2003).
  - [7] E. Dagotto *et al.*, Phys. Rep. **344**, 1 (2001); Y. Tokura and Y. Tomioka, J. Magn. Magn. Mater. **200**, 1 (1999).
  - [8] V.N. Smolyaninova *et al.*, Phys. Rev. B **65**, 104419

- (2002); M.S. Reis *et al.*, *ibid* **71**, 144413 (2005).
- [9] P.G. Radaelli *et al.*, Phys. Rev. B **63**, 172419 (2001).
- [10] D. Saurel *et al.*, Phys. Rev. B **73**, 094438 (2006); S. Mercone *et al.*, *ibid* **68**, 094422 (2003).
- [11] A tiny magnetic contribution was found in the clean STO substrates. This could be due to 1-2 ppm of Fe impurities that are present even in the best STO crystals available.
- [12] D. Niebieskikwiat *et al.*, J. Magn. Magn. Mater. **237**, 241 (2001); Phys. Rev. B **63**, 212402 (2001).
- [13] S.S.P. Parkin *et al.*, Phys. Rev. Lett. **64**, 2304 (1990); C.F. Majkrzak *et al.*, *ibid* **56**, 2700 (1986).
- [14] A. Hoffmann *et al.*, Phys. Rev. B **72**, 140407(R) (2005); S. Park *et al.*, *ibid* **70**, 104406 (2004); J.A.C. Bland *et al.*, *ibid* **57**, 10272 (1998).
- [15] J. Chakhalian *et al.*, Nat. Phys. **2**, 244 (2006).
- [16] P.A. Kienzle *et al.*, <http://www.ncnr.nist.gov/reflpak>, 2000-2006.
- [17] J.-H. Park *et al.*, Phys. Rev. Lett. **81**, 1953 (1998).
- [18] J.W. Freeland *et al.*, Nat. Mater. **4**, 62 (2005).
- [19] I. Panagiotopoulos *et al.*, J. Appl. Phys. **85**, 4913 (1999).
- [20] J. Tao *et al.*, Phys. Rev. Lett. **94**, 147206 (2005); M. Bibes *et al.*, *ibid* **87**, 067210 (2001).
- [21] M. Izumi *et al.*, Phys. Rev. B **61**, 12187 (2000).